PHYSICAL REVIEW A **81**, 063834 (2010)

Quadripartite continuous-variable entanglement via quadruply concurrent down-conversion

S. L. W. Midgley,[1] A. S. Bradley,[2] O. Pfister,[3] and M. K. Olsen[1]
[1]*ARC Centre of Excellence for Quantum-Atom Optics, School of Mathematics and Physics, University of Queensland, QLD 4072, Australia*
[2]*Jack Dodd Centre for Quantum Technology, Department of Physics, University of Otago, Post Office Box 56, Dunedin, New Zealand*
[3]*Department of Physics, University of Virginia, 382 McCormick Road, Charlottesville, Virginia 22904-4714, USA*
(Received 8 February 2010; published 30 June 2010)

We investigate an experimentally feasible intracavity coupled down-conversion scheme to generate quadripartite entanglement using concurrent nonlinearities. We verify that quadripartite entanglement is present in this system by calculating the output fluctuation spectra and then considering violations of optimized inequalities of the van Loock–Furusawa type. The entanglement characteristics both above and below the oscillation threshold are considered. We also present analytic solutions for the quadrature operators and the van Loock–Furusawa correlations in the undepleted pump approximation.

DOI: 10.1103/PhysRevA.81.063834 PACS number(s): 42.50.Dv, 42.65.Lm, 03.65.Ud, 03.67.Mn

I. INTRODUCTION

Entanglement is a concept of central importance in quantum theory and continues to inspire both theoretical and experimental efforts to explore quantum systems. In addition to this, entanglement is the main resource of quantum information and in particular, multipartite continuous-variable (CV) entangled states have grown to be pivotal in multipartite quantum communication [1–7]. The criteria which must be satisfied to establish whether bipartite entanglement exists in a given system are well known for the CV case [8,9]. Furthermore, bipartite entanglement can be realized experimentally. The criteria for the bipartite scenario have been generalized for multipartite entanglement by van Loock and Furusawa [10]. Advances have also taken place in the experimental generation of tripartite entanglement. In particular, there have been experiments where entangled beams are produced by mixing squeezed beams with linear optics [2,4,5,7,11,12]. Several proposals have also been made whereby multifrequency entangled outputs are generated. These rely on the use of nondegenerate down-conversion [13] or cascaded or concurrent nonlinear optical processes [14–19] where the tripartite entanglement is instead produced via the interaction with the nonlinear medium itself. It is these concurrent processes that we consider in this work for the quadripartite case.

In regards to quadripartite entangled beams, there have been theoretical proposals based on linear optics and cascaded nonlinearites [20–23]. In this work we build on a tripartite scheme proposed by Bradley *et al.* in [17] but for the case of quadruply concurrent nonlinearities. Furthermore, we use an optimized version of the van Loock–Furusawa inequalities to demonstrate quadripartite entanglement in this system.

This article is organized as follows. In Sec. II we describe the Hamiltonian and the physical system under consideration. Section III discusses the van Loock–Furusawa (VLF) criteria as a means of quantifying quadripartite entanglement. Section IV considers the interaction Hamiltonian in the undepleted pump approximation and gives analytic solutions for the quadrature operators, as well as the VLF correlations. In Sec. V we present the full equations of motion for the system and Sec. VI gives the steady-state solutions to the classical versions of the equations of motion and provides an overview of the linearized fluctuation analysis used in this work to calculate the measurable output fluctuation spectra from the cavity. These output spectra are are found in Sec. VII and used to demonstrate violation of the optimized VLF criteria and, hence, demonstrate quadripartite entanglement.

II. SYSTEM AND HAMILTONIAN

We model a system in which pump lasers drive four modes in an optical cavity. As depicted in the simplified experimental setup shown in Fig. 1, the four inputs interact with a $\chi^{(2)}$ nonlinear crystal to produce four low-frequency entangled output beams at frequencies ω_5, ω_6, ω_7, and ω_8. For example, mode 1 is pumped at a particular frequency and polarization such that it produces modes 5 and 6.

This is an experimentally feasible system. The reader will find very concrete and detailed experimental proposals in [14,24–26] for quadripartite states and in [27,28] for a much more complex, scalable cluster state suitable for universal quantum computing [29]. Note also that the required nonlinear media [26,27] have been experimentally demonstrated in quasi-phase-matched $KTiOPO_4$ [25] and their optimized and sophisticated engineering has recently been experimentally validated [30].

The full Hamiltonian for the eight-mode system, describing the interaction inside the optical cavity and the interaction of the cavity fields with the output fields, can be written as

$$\mathcal{H} = \mathcal{H}_{\rm pump} + \mathcal{H}_{\rm int} + \mathcal{H}_{\rm free} + \mathcal{H}_{\rm res}, \tag{1}$$

where the interaction Hamiltonian is

$$\mathcal{H}_{\rm int} = i\hbar[\chi_1\hat{a}_1\hat{a}_5^\dagger\hat{a}_6^\dagger + \chi_2\hat{a}_2\hat{a}_6^\dagger\hat{a}_7^\dagger + \chi_3\hat{a}_3\hat{a}_7^\dagger\hat{a}_8^\dagger + \chi_4\hat{a}_4\hat{a}_8^\dagger\hat{a}_5^\dagger] + \text{H.c.}, \tag{2}$$

with the χ_i representing the effective nonlinearities and $\hat{a}_i$ denoting the bosonic annihilation operators for the intracavity modes at frequencies ω_i. The pumping Hamiltonian, describing the cavity driving fields, in the appropriate rotating frame is

$$\mathcal{H}_{\rm pump} = i\hbar\sum_{i=1}^{4}[\epsilon_i\hat{a}_i^\dagger - \epsilon_i^*\hat{a}_i], \tag{3}$$

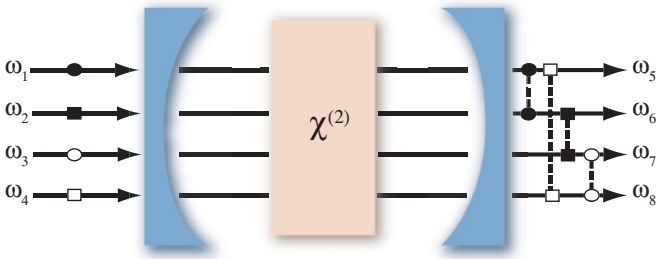

FIG. 1. (Color online) Schematic of a $\chi^{(2)}$ crystal inside a pumped Fabry-Pérot cavity. Pump lasers drive four intracavity modes with frequencies ω_1, ω_2, ω_3, and ω_4 (represented by circles and squares), which are down-converted to four output modes with frequencies ω_5, ω_6, ω_7, and ω_8.

and the cavity damping Hamiltonian is given by

$$\mathcal{H}_{\rm res} = \hbar \sum_{i=1}^{8} [\hat{\Gamma}_i \hat{a}_i^\dagger + \hat{\Gamma}_i^\dagger \hat{a}_i], \tag{4}$$

where ϵ_i are the classical pumping laser amplitudes for mode i and the $\hat{\Gamma}_i$ are the annihilation operators for bath quanta to which each of the intracavity modes are coupled and which represent losses through the cavity mirror.

III. QUADRIPARTITE ENTANGLEMENT MEASURES

In order to investigate multipartite entanglement, and in particular show that the system under consideration demonstrates true quadripartite entanglement, we first define quadrature operators [31] for each mode as

$$\hat{X}_i = \hat{a}_i + \hat{a}_i^\dagger, \quad \hat{Y}_i = -i(\hat{a}_i - \hat{a}_i^\dagger), \tag{5}$$

such that $[\hat{X}_i, \hat{Y}_i] = 2i$. Based on this definition $V(\hat{X}_i) \geqslant 1$, for example, indicates single-mode squeezing, where $V(\hat{A}) = \langle \hat{A}^2 \rangle - \langle \hat{A} \rangle^2$ denotes the variance. The conditions proposed by van Loock and Furusawa [10], which are a generalization of the conditions for bipartite entanglement [8,9], are sufficient to demonstrate multipartite entanglement. We now demonstrate how these may be optimized for the verification of genuine quadripartite entanglement in this system.

Using the quadrature definitions in Eq. (5), the quadripartite inequalities which must be simultaneously violated by the low frequency modes are

$$V(\hat{X}_5 - \hat{X}_6) + V(\hat{Y}_5 + \hat{Y}_6 + g_7 \hat{Y}_7 + g_8 \hat{Y}_8) \geqslant 4, \tag{6}$$

$$V(\hat{X}_6 - \hat{X}_7) + V(g_5 \hat{Y}_5 + \hat{Y}_6 + \hat{Y}_7 + g_8 \hat{Y}_8) \geqslant 4, \tag{7}$$

$$V(\hat{X}_7 - \hat{X}_8) + V(g_5 \hat{Y}_5 + g_6 \hat{Y}_6 + \hat{Y}_7 + \hat{Y}_8) \geqslant 4, \tag{8}$$

where the $g_i (i = 5,6,7,8)$ are arbitrary real parameters that are used to optimize the violation of these inequalities. In particular, we minimize Eqs. (6) and (8) with respect to $g_{7,8}$ and $g_{5,6}$, respectively. Solving the resulting equations leads to the optimized expressions

$$g_5 = \frac{V_6(V_{57} + V_{58}) - V_{56}(V_{67} + V_{68})}{V_{56}^2 - V_5 V_6}, \tag{9}$$

$$g_6 = \frac{V_5(V_{67} + V_{68}) - V_{56}(V_{57} + V_{58})}{V_{56}^2 - V_5 V_6}, \tag{10}$$

$$g_7 = \frac{V_8(V_{57} + V_{67}) - V_{78}(V_{58} + V_{68})}{V_{78}^2 - V_7 V_8}, \tag{11}$$

$$g_8 = \frac{V_7(V_{58} + V_{68}) - V_{78}(V_{57} + V_{67})}{V_{78}^2 - V_7 V_8}, \tag{12}$$

where for covariances we use the notation $V_{ij} = (\langle \hat{Y}_i \hat{Y}_j \rangle + \langle \hat{Y}_j \hat{Y}_i \rangle)/2 - \langle \hat{Y}_i \rangle \langle \hat{Y}_j \rangle$ and for the case where $i = j$ the covariance, denoted V_i, reduces to the usual variance, $V(\hat{Y}_i)$. It is important to note that in the uncorrelated limit these optimized VLF criteria approach 4. Hence, without optimization, some entanglement which is present may be missed.

IV. ANALYTIC SOLUTIONS IN THE UNDEPLETED PUMP APPROXIMATION

It is useful to consider the interaction Hamiltonian in the undepleted pump approximation in the absence of a cavity in advance of a more complete approach that considers the full quantum equations of motion for all of the interacting fields inside a cavity. We stress here that these equations are not of exact physical relevance but do give useful insights into the properties of the Hamiltonian. Here we show that it is possible to obtain analytic solutions for the quadrature operator equations of motion using the undepleted pump approximation. This entails setting $\xi_i = \chi_i \langle \hat{a}_i(0) \rangle$ $(i = 1,2,3,4)$, where ξ_i are positive, real constants. Under these conditions, the interaction Hamiltonian can be written as

$$\mathcal{H}_{\rm int} = i\hbar[\xi_1(\hat{a}_5^\dagger \hat{a}_6^\dagger - \hat{a}_5 \hat{a}_6) + \xi_2(\hat{a}_6^\dagger \hat{a}_7^\dagger - \hat{a}_6 \hat{a}_7) + \xi_3(\hat{a}_7^\dagger \hat{a}_8^\dagger - \hat{a}_7 \hat{a}_8) + \xi_4(\hat{a}_8^\dagger \hat{a}_5^\dagger - \hat{a}_8 \hat{a}_5)]. \tag{13}$$

The Heisenberg equations of motion can then be written

$$\frac{d\hat{a}_5}{dt} = \xi_1 \hat{a}_6^\dagger + \xi_4 \hat{a}_8^\dagger, \tag{14}$$

$$\frac{d\hat{a}_6}{dt} = \xi_1 \hat{a}_5^\dagger + \xi_2 \hat{a}_7^\dagger, \tag{15}$$

$$\frac{d\hat{a}_7}{dt} = \xi_2 \hat{a}_6^\dagger + \xi_3 \hat{a}_8^\dagger, \tag{16}$$

$$\frac{d\hat{a}_8}{dt} = \xi_3 \hat{a}_7^\dagger + \xi_4 \hat{a}_5^\dagger, \tag{17}$$

and these equations can be recast in terms of the quadrature operators as follows:

$$\frac{d\hat{X}_5}{dt} = \xi_1 \hat{X}_6 + \xi_4 \hat{X}_8, \tag{18}$$

$$\frac{d\hat{Y}_5}{dt} = -\xi_1 \hat{Y}_6 - \xi_4 \hat{Y}_8, \tag{19}$$

$$\frac{d\hat{X}_6}{dt} = \xi_1 \hat{X}_5 + \xi_2 \hat{X}_7, \tag{20}$$

$$\frac{d\hat{Y}_6}{dt} = -\xi_1 \hat{Y}_5 - \xi_2 \hat{Y}_7, \tag{21}$$

$$\frac{d\hat{X}_7}{dt} = \xi_2 \hat{X}_6 + \xi_3 \hat{X}_8, \tag{22}$$

$$\frac{d\hat{Y}_7}{dt} = -\xi_2\hat{Y}_6 - \xi_3\hat{Y}_8, \tag{23}$$

$$\frac{d\hat{X}_8}{dt} = \xi_3\hat{X}_7 + \xi_4\hat{X}_5, \tag{24}$$

$$\frac{d\hat{Y}_8}{dt} = -\xi_3\hat{Y}_7 - \xi_4\hat{Y}_5. \tag{25}$$

These are the equations that we solve to find analytic solutions for the quadrature operators as functions of their initial values.

A. Solutions with equal ξ_i

To begin with, we set all the interactions equal so that $\xi_i = \xi$ and find analytic expressions for the VLF correlations by solving the Heisenberg equations of motion for this case. The solutions for the quadrature operators are found to be

$$\hat{X}_5(t) = A\hat{X}_5(0) + B\hat{X}_6(0) + C\hat{X}_7(0) + B\hat{X}_8(0), \tag{26}$$

$$\hat{Y}_5(t) = A\hat{Y}_5(0) - B\hat{Y}_6(0) + C\hat{Y}_7(0) - B\hat{Y}_8(0), \tag{27}$$

$$\hat{X}_6(t) = B\hat{X}_5(0) + A\hat{X}_6(0) + B\hat{X}_7(0) + C\hat{X}_8(0), \tag{28}$$

$$\hat{Y}_6(t) = -B\hat{Y}_5(0) + A\hat{Y}_6(0) - B\hat{Y}_7(0) + C\hat{Y}_8(0), \tag{29}$$

$$\hat{X}_7(t) = C\hat{X}_5(0) + B\hat{X}_6(0) + A\hat{X}_7(0) + B\hat{X}_8(0), \tag{30}$$

$$\hat{Y}_7(t) = C\hat{Y}_5(0) - B\hat{Y}_6(0) + A\hat{Y}_7(0) - B\hat{Y}_8(0), \tag{31}$$

$$\hat{X}_8(t) = B\hat{X}_5(0) + C\hat{X}_6(0) + B\hat{X}_7(0) + A\hat{X}_8(0), \tag{32}$$

$$\hat{Y}_8(t) = -B\hat{Y}_5(0) + C\hat{Y}_6(0) - B\hat{Y}_7(0) + A\hat{Y}_8(0), \tag{33}$$

where

$$A = \cosh^2(\xi t), \tag{34}$$

$$B = \tfrac{1}{2}\sinh(2\xi t), \tag{35}$$

$$C = \sinh^2(\xi t). \tag{36}$$

From these expressions for the quadrature operators it is possible to find the variances and covariances necessary to calculate the VLF criteria within the undepleted pump approximation. In fact, the variances are all equal and given by the following time-dependent moments:

$$\langle\hat{X}_i^2\rangle = \langle\hat{Y}_i^2\rangle = A^2 + 2B^2 + C^2, \tag{37}$$

since the expectation values of the amplitudes are all zero. Here we have used the fact that $\langle\hat{X}_i(0)\hat{X}_j(0)\rangle = \langle\hat{Y}_i(0)\hat{Y}_j(0)\rangle = \delta_{ij}$. A similar approach can be used to calculate the covariances which are equivalent to the time-dependent moments $\langle\hat{X}_i\hat{X}_j\rangle$ and $\langle\hat{Y}_i\hat{Y}_j\rangle$. In particular, the covariances are given by

$$\langle\hat{X}_5X_6\rangle = -\langle\hat{Y}_5Y_6\rangle = 2(AB + BC), \tag{38}$$

$$\langle\hat{X}_5X_7\rangle = \langle\hat{Y}_5Y_7\rangle = 2(AC + B^2), \tag{39}$$

$$\langle\hat{X}_5X_8\rangle = -\langle\hat{Y}_5Y_8\rangle = 2(AB + BC), \tag{40}$$

$$\langle\hat{X}_6X_7\rangle = -\langle\hat{Y}_6Y_7\rangle = 2(AB + BC), \tag{41}$$

$$\langle\hat{X}_6X_8\rangle = \langle\hat{Y}_6Y_8\rangle = 2(AC + B^2), \tag{42}$$

$$\langle\hat{X}_7X_8\rangle = -\langle\hat{Y}_7Y_8\rangle = 2(AB + BC). \tag{43}$$

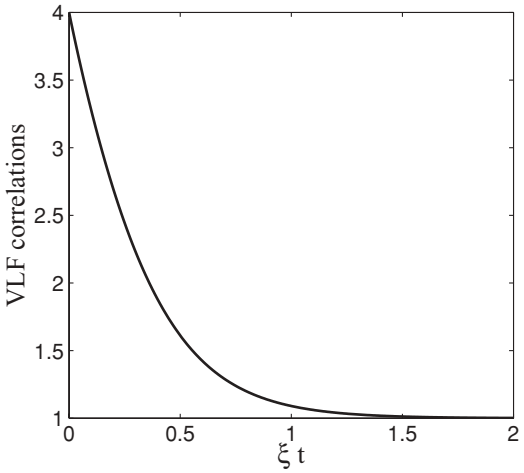

FIG. 2. Analytic solutions for the optimized van Loock–Furusawa correlations, V_3, found by solving the Heisenberg equations of motion in the undepleted pump approximation. A value of less than 4 signifies quadripartite entanglement. All quantities depicted here, and in subsequent graphs, are dimensionless.

From these variances and covariances we obtain Eq. (44), an analytic expression for the optimized VLF correlations defined in Eqs. (6)–(8). All three VLF correlations are equal when $\xi_i = \xi$, and hence we label any of the correlations in Eqs. (6)–(8) as V_3. Figure 2 provides a plot of these optimized VLF correlations, V_3, as a function of ξt.

$$V_3 = 4A^2 - 4A\sqrt{2B} + 4(\sqrt{2B} - C)C + \frac{2(B^2 - 4B^{3/2}C\sqrt{2} + 12BC^2 - 8C^3\sqrt{2B} + 4C^4)}{A^2 - 2A\sqrt{B} + B - C\sqrt{2B} + C^2}. \tag{44}$$

We observe that quadripartite entanglement is present in this system, with $V_3 < 4$ for all ξt. This suggests a more complete treatment incorporating depletion of the pump fields and a cavity will find where quadripartite entanglement is present.

B. Solutions with unequal ξ_i

For simplicity, here we assume that $\xi_1 = \xi_2$ and $\xi_3 = \xi_4$, and setting $\Omega = \sqrt{\xi_1^2 + \xi_3^2}$ we find that the solutions are given by

$$\hat{X}_5(t) = D\hat{X}_5(0) + E\hat{X}_6(0) + F\hat{X}_7(0) + G\hat{X}_8(0), \tag{45}$$

$$\hat{Y}_5(t) = D\hat{Y}_5(0) - E\hat{Y}_6(0) + F\hat{Y}_7(0) - G\hat{Y}_8(0), \tag{46}$$

$$\hat{X}_6(t) = E\hat{X}_5(0) + H\hat{X}_6(0) + E\hat{X}_7(0) + I\hat{X}_8(0), \tag{47}$$

$$\hat{Y}_6(t) = -E\hat{Y}_5(0) + H\hat{Y}_6(0) - E\hat{Y}_7(0) + I\hat{Y}_8(0), \tag{48}$$

$$\hat{X}_7(t) = F\hat{X}_5(0) + E\hat{X}_6(0) + D\hat{X}_7(0) + G\hat{X}_8(0), \tag{49}$$

$$\hat{Y}_7(t) = F\hat{Y}_5(0) - E\hat{Y}_6(0) + D\hat{Y}_7(0) - G\hat{Y}_8(0), \tag{50}$$

$$\hat{X}_8(t) = G\hat{X}_5(0) + I\hat{X}_6(0) + G\hat{X}_7(0) + J\hat{X}_8(0), \tag{51}$$

$$\hat{Y}_8(t) = -G\hat{Y}_5(0) + I\hat{Y}_6(0) - G\hat{Y}_7(0) + J\hat{Y}_8(0), \tag{52}$$

where

$$D = \cosh^2(\Omega t/\sqrt{2}), \tag{53}$$

$$E = \sinh^2(\Omega t/\sqrt{2}), \tag{54}$$

$$F = \frac{\xi_1 \sinh(\sqrt{2}\Omega t)}{\sqrt{2}\Omega}, \tag{55}$$

$$G = \frac{\xi_3 \sinh(\sqrt{2}\Omega t)}{\sqrt{2}\Omega}, \tag{56}$$

$$H = \frac{\xi_3^2 + \xi_1^2 \cosh(\sqrt{2}\Omega t)}{\Omega^2}, \tag{57}$$

$$I = \frac{\xi_1\xi_3[\cosh(\sqrt{2}\Omega t) - 1]}{\Omega^2}, \tag{58}$$

$$J = \frac{\xi_1^2 + \xi_3^2 \cosh(\sqrt{2}\Omega t)}{\Omega^2}. \tag{59}$$

We note here the generality of the solutions presented and that other cases are possible numerically. The variances are given by

$$\langle \hat{X}_5^2 \rangle = \langle \hat{Y}_5^2 \rangle = D^2 + E^2 + F^2 + G^2, \tag{60}$$

$$\langle \hat{X}_6^2 \rangle = \langle \hat{Y}_6^2 \rangle = 2E^2 + H^2 + I^2, \tag{61}$$

$$\langle \hat{X}_7^2 \rangle = \langle \hat{Y}_7^2 \rangle = D^2 + E^2 + F^2 + G^2, \tag{62}$$

$$\langle \hat{X}_8^2 \rangle = \langle \hat{Y}_8^2 \rangle = 2G^2 + I^2 + J^2, \tag{63}$$

and the covariances are

$$\langle \hat{X}_5 X_6 \rangle = -\langle \hat{Y}_5 Y_6 \rangle = DE + EH + EF + IG, \tag{64}$$

$$\langle \hat{X}_5 X_7 \rangle = \langle \hat{Y}_5 Y_7 \rangle = 2DF + E^2 + G^2, \tag{65}$$

$$\langle \hat{X}_5 X_8 \rangle = -\langle \hat{Y}_5 Y_8 \rangle = DG + EI + FG + GJ, \tag{66}$$

$$\langle \hat{X}_6 X_7 \rangle = -\langle \hat{Y}_6 Y_7 \rangle = DE + EH + EF + IG, \tag{67}$$

$$\langle \hat{X}_6 X_8 \rangle = \langle \hat{Y}_6 Y_8 \rangle = 2EG + HI + IJ, \tag{68}$$

$$\langle \hat{X}_7 X_8 \rangle = -\langle \hat{Y}_7 Y_8 \rangle = DG + EI + FG + GJ. \tag{69}$$

As described in Sec. IV A, we can now calculate the VLF correlations. Figure 3 shows the optimized VLF correlations as a function of $\xi_1 t$, for the case $\xi_3 = 0.5\xi_1$. Again, we observe that quadripartite entanglement is present in this system with all three VLF correlations less than 4 for some $\xi_1 t$. Comparing Figs. 2 and 3 we see that the greatest degree of entanglement is obtained for the case where all ξ_i are equal. Figure 3 shows that for each VLF correlation the entanglement is degraded beyond a particular value of $\xi_1 t$; however, this is not the case in Fig. 2 when all the ξ_i are equal.

V. EQUATIONS OF MOTION FOR THE FULL HAMILTONIAN

We now consider the full physical system, where the nonlinear media are contained inside a pumped resonant Fabry-Pérot cavity. The master equation for the density operator of the system can be found in the standard manner by tracing over the reservoirs [32] and is given by

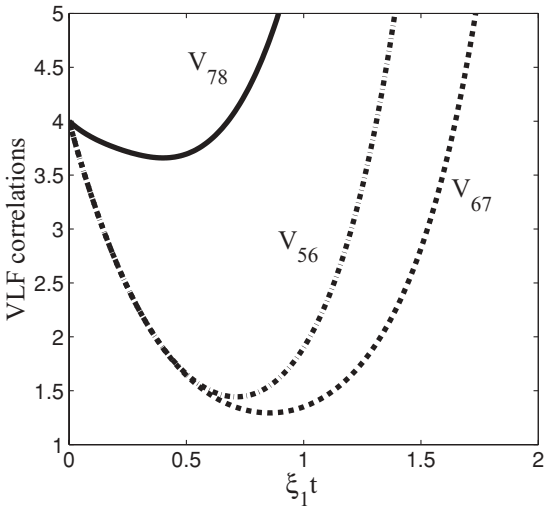

FIG. 3. Analytic solutions for the optimized van Loock–Furusawa correlations, V_{56}, V_{67}, and V_{78} with $\xi_3 = 0.5\xi_1$, found by solving the Heisenberg equations of motion in the undepleted pump approximation. Having all three of the correlations drop below 4 is sufficient to demonstrate quadripartite entanglement.

$$\frac{\partial \hat{\rho}}{\partial t} = -\frac{i}{\hbar}[\hat{H}_{\text{pump}} + \hat{H}_{\text{int}}, \hat{\rho}] + \sum_{i=1}^{8} \gamma_i \mathcal{D}_i[\hat{\rho}], \tag{70}$$

where γ_i are the cavity loss rates at the respective frequencies and $\mathcal{D}_i[\hat{\rho}] = 2\hat{a}_i\hat{\rho}\hat{a}_i^\dagger - \hat{a}_i^\dagger\hat{a}_i\hat{\rho} - \hat{\rho}\hat{a}_i^\dagger\hat{a}_i$ is the Lindblad superoperator [32] under the usual zero-temperature Markov approximation. From this one can derive the stochastic differential equations (SDEs) in the positive-P representation [33] and, in turn, study the intracavity dynamics.

Our approach [34] involves converting the quantum operator equations of motion of Eq. (70) into a Fokker-Planck equation for the positive-P representation pseudoprobability distribution of the system [33,34]. This can then be interpreted as a set of c-number SDEs. It should be noted that the use of the positive-P representation, rather than the Glauber-Sudarshan P representation [35,36], is necessary to ensure that the diffusion matrix of the FPE is positive-definite. This is achieved with the positive-P approach by defining two independent stochastic fields α_i and α_i^+ corresponding to the mode operators $\hat{a}_i$ and $\hat{a}_i^\dagger$, respectively, in the limit of a large number of stochastic trajectories. Using this method it is possible to calculate stochastic trajectory averages which correspond to the normally ordered expectation values of quantum-mechanical operators, for example, $\overline{(\alpha_i)^n(\alpha_j^+)^m} = \langle(\hat{a}_j^\dagger)^m\hat{a}_i^n\rangle$. Taking this approach yields a diffusion matrix of the form

$$\boldsymbol{D} = \begin{pmatrix} \mathbf{0} & \mathbf{0} \\ \mathbf{0} & \boldsymbol{d} \end{pmatrix}, \tag{71}$$

where $\mathbf{0}$ is an 8×8 null matrix and the nonzero block is given by

$$\boldsymbol{d} = \begin{pmatrix} 0 & 0 & \chi_1\alpha_1 & 0 & 0 & 0 & \chi_4\alpha_4 & 0 \\ 0 & 0 & 0 & \chi_1\alpha_1^+ & 0 & 0 & 0 & \chi_4\alpha_4^+ \\ \chi_1\alpha_1 & 0 & 0 & 0 & \chi_2\alpha_2 & 0 & 0 & 0 \\ 0 & \chi_1\alpha_1^+ & 0 & 0 & 0 & \chi_2\alpha_2^+ & 0 & 0 \\ 0 & 0 & \chi_2\alpha_2 & 0 & 0 & 0 & \chi_3\alpha_3 & 0 \\ 0 & 0 & 0 & \chi_2\alpha_2^+ & 0 & 0 & 0 & \chi_3\alpha_3^+ \\ \chi_4\alpha_4 & 0 & 0 & 0 & \chi_3\alpha_3 & 0 & 0 & 0 \\ 0 & \chi_4\alpha_4^+ & 0 & 0 & 0 & \chi_3\alpha_3^+ & 0 & 0 \end{pmatrix}. \tag{72}$$

The matrix $\boldsymbol{d}$ can be factorized such that the Itô SDEs are obtained. For the high-frequency fields, this process yields

$$\begin{aligned} \frac{d\alpha_1}{dt} &= \epsilon_1 - \chi_1\alpha_5\alpha_6 - \gamma_1\alpha_1, \\ \frac{d\alpha_2}{dt} &= \epsilon_2 - \chi_2\alpha_6\alpha_7 - \gamma_2\alpha_2, \\ \frac{d\alpha_3}{dt} &= \epsilon_3 - \chi_3\alpha_7\alpha_8 - \gamma_3\alpha_3, \\ \frac{d\alpha_4}{dt} &= \epsilon_4 - \chi_4\alpha_8\alpha_5 - \gamma_4\alpha_4, \end{aligned} \tag{73}$$

and also the equations found by interchanging α_i and α_i^+. While for the low-frequency fields, one obtains

$$\begin{aligned} \frac{d\alpha_5}{dt} &= \chi_1\alpha_1\alpha_6^+ + \chi_4\alpha_4\alpha_8^+ - \gamma_5\alpha_5 + \sqrt{\frac{\chi_1\alpha_1}{2}}[\eta_5(t) + i\eta_6(t)] \\ &\quad + \sqrt{\frac{\chi_4\alpha_4}{2}}[\eta_{13}(t) + i\eta_{14}(t)], \\ \frac{d\alpha_6}{dt} &= \chi_1\alpha_1\alpha_5^+ + \chi_2\alpha_2\alpha_7^+ - \gamma_6\alpha_6 + \sqrt{\frac{\chi_1\alpha_1}{2}}[\eta_5(t) - i\eta_6(t)] \\ &\quad + \sqrt{\frac{\chi_2\alpha_2}{2}}[\eta_9(t) + i\eta_{10}(t)], \\ \frac{d\alpha_7}{dt} &= \chi_2\alpha_2\alpha_6^+ + \chi_3\alpha_3\alpha_8^+ - \gamma_7\alpha_7 + \sqrt{\frac{\chi_3\alpha_3}{2}}[\eta_1(t) + i\eta_2(t)] \\ &\quad + \sqrt{\frac{\chi_2\alpha_2}{2}}[\eta_9(t) - i\eta_{10}(t)], \\ \frac{d\alpha_8}{dt} &= \chi_3\alpha_3\alpha_7^+ + \chi_4\alpha_4\alpha_5^+ - \gamma_8\alpha_8 + \sqrt{\frac{\chi_3\alpha_3}{3}}[\eta_1(t) - i\eta_2(t)] \\ &\quad + \sqrt{\frac{\chi_4\alpha_4}{2}}[\eta_{13}(t) - i\eta_{14}(t)], \end{aligned} \tag{74}$$

and also the equations found by interchanging α_i and α_i^+ and $\eta_i(t)$ and $\eta_{i+2}(t)$. The γ_i are the cavity loss rates at the respective frequencies, and $\eta_i(t)$ are real, independent, Gaussian noise terms which satisfy $\overline{\eta_i(t)} = 0$ and $\overline{\eta_i(t)\eta_j(t')} = \delta_{ij}\delta(t - t')$. It should be mentioned that we are assuming that all the intracavity modes are resonant with the cavity, and although it is possible to include detuning, we do not do so here.

VI. STABILITY ANALYSIS AND FLUCTUATION SPECTRA

We conduct a linearized fluctuation analysis [32] of the system for the purposes of calculating the output spectral correlations for the cavity from the intracavity spectra. We begin by neglecting the noise terms in Eq. (74) so that $\alpha_i^+ \to \alpha_i^*$ and also set $\alpha_i = \bar{\alpha}_i + \delta\alpha_i$, where $\bar{\alpha}_i$ is a mean value and $\delta\alpha_i$ represents the fluctuations. This gives a set of classical equations for the mean values:

$$\begin{aligned} \frac{d\bar{\alpha}_1}{dt} &= \epsilon_1 - \chi_1\bar{\alpha}_5\bar{\alpha}_6 - \gamma_1\bar{\alpha}_1, \\ \frac{d\bar{\alpha}_2}{dt} &= \epsilon_2 - \chi_2\bar{\alpha}_6\bar{\alpha}_7 - \gamma_2\bar{\alpha}_2, \\ \frac{d\bar{\alpha}_3}{dt} &= \epsilon_3 - \chi_3\bar{\alpha}_7\bar{\alpha}_8 - \gamma_3\bar{\alpha}_3, \\ \frac{d\bar{\alpha}_4}{dt} &= \epsilon_4 - \chi_4\bar{\alpha}_8\bar{\alpha}_5 - \gamma_4\bar{\alpha}_4, \\ \frac{d\bar{\alpha}_5}{dt} &= \chi_1\bar{\alpha}_1\bar{\alpha}_6^* + \chi_4\bar{\alpha}_4\bar{\alpha}_8^* - \gamma_5\bar{\alpha}_5, \\ \frac{d\bar{\alpha}_6}{dt} &= \chi_1\bar{\alpha}_1\bar{\alpha}_5^* + \chi_2\bar{\alpha}_2\bar{\alpha}_7^* - \gamma_6\bar{\alpha}_6, \\ \frac{d\bar{\alpha}_7}{dt} &= \chi_2\bar{\alpha}_2\bar{\alpha}_6^* + \chi_3\bar{\alpha}_3\bar{\alpha}_8^* - \gamma_7\bar{\alpha}_7, \\ \frac{d\bar{\alpha}_8}{dt} &= \chi_3\bar{\alpha}_3\bar{\alpha}_7^* + \chi_4\bar{\alpha}_4\bar{\alpha}_5^* - \gamma_8\bar{\alpha}_8, \end{aligned} \tag{75}$$

and from these we can obtain steady-state solutions.

In the remainder of this article we consider a symmetric system where all the high-frequency modes have the same cavity-damping rates, with $\gamma_i = \gamma$ for $i = 1,2,3,4$ and all low-frequency modes also have equal cavity-damping rates, with $\gamma_i = \kappa$ for $i = 5,6,7,8$. In addition to this, we assume that all the nonlinearities and hence all the pump field amplitudes are equal; that is, $\chi_i = \chi$ and $\epsilon_i = \epsilon$, respectively.

For this completely symmetric system, we verify that there is an oscillation threshold at the critical pumping amplitude,

$$\epsilon_c = \frac{\gamma\kappa}{2\chi}, \tag{76}$$

as is the case for triply concurrent down-conversion [17]. This result differs from the standard nondegenerate optical parametric oscillator (OPO) threshold condition by a factor of a half. This difference here is due to the fact that each pump

mode drives two down-conversion processes. The stationary solutions below this threshold value are found to be

$$\begin{aligned} \bar{\alpha}_i &= \frac{\epsilon}{\gamma} \quad \text{for} \quad i \in \{1,2,3,4\}, \\ \bar{\alpha}_i &= 0 \quad \text{for} \quad i \in \{5,6,7,8\}, \end{aligned} \tag{77}$$

while above threshold the stationary solutions are given by

$$\bar{\alpha}_i = \frac{\kappa}{2\chi} \quad \text{for} \quad i \in \{1,2,3,4\}, \tag{78}$$

$$\bar{\alpha}_i = \sqrt{(\epsilon - \epsilon_c)/\chi} \quad \text{for} \quad i \in \{5,6,7,8\}. \tag{79}$$

We see that the low-frequency modes become macroscopically occupied as the pumping is increased and the high-frequency modes remain at their threshold value. Using Eqs. (73) and (74), we also perform dynamical simulations to confirm the steady-state values.

We then proceed to study fluctuations around the steady state which allows one to calculate measurable output fluctuation spectra [34] and, hence, quantify the quantum correlations of the system. The linearized equations for the fluctuations are of the form

$$d\boldsymbol{\delta\alpha} = -\bar{\boldsymbol{A}}\boldsymbol{\delta\alpha}dt + \bar{\boldsymbol{B}}d\boldsymbol{W}, \tag{80}$$

where $\boldsymbol{\delta\alpha} = [\delta\alpha_1, \delta\alpha_1^+, \delta\alpha_2, \delta\alpha_2^+, \ldots, \delta\alpha_8, \delta\alpha_8^+]^T$, $\bar{\boldsymbol{B}}$ is the noise matrix of Eq. (74) with the steady-state values inserted, $d\boldsymbol{W}$ is a vector of independent, real Wiener increments [34], and $\bar{\boldsymbol{A}}$ is the drift matrix with the steady-state values inserted and given by

$$\bar{\boldsymbol{A}} = \begin{pmatrix} \boldsymbol{A}_1 & \boldsymbol{A}_2 \\ -(\boldsymbol{A}_2^*)^T & \boldsymbol{A}_3 \end{pmatrix}, \tag{81}$$

where $\boldsymbol{A}_1 = -\gamma I_6$,

$$\boldsymbol{A}_2 = \begin{pmatrix} -\chi_1\bar{\alpha}_6 & 0 & -\chi_1\bar{\alpha}_5 & 0 & 0 & 0 & 0 & 0 \\ 0 & -\chi_1\bar{\alpha}_6^* & 0 & -\chi_1\bar{\alpha}_5^* & 0 & 0 & 0 & 0 \\ 0 & 0 & -\chi_2\bar{\alpha}_7 & 0 & -\chi_2\bar{\alpha}_6 & 0 & 0 & 0 \\ 0 & 0 & 0 & -\chi_2\bar{\alpha}_7^* & 0 & -\chi_2\bar{\alpha}_6^* & 0 & 0 \\ 0 & 0 & 0 & 0 & -\chi_3\bar{\alpha}_8 & 0 & -\chi_3\bar{\alpha}_7 & 0 \\ 0 & 0 & 0 & 0 & 0 & -\chi_3\bar{\alpha}_8^* & 0 & -\chi_3\bar{\alpha}_7^* \\ -\chi_4\bar{\alpha}_8 & 0 & 0 & 0 & 0 & 0 & -\chi_4\bar{\alpha}_5 & 0 \\ 0 & -\chi_4\bar{\alpha}_8^* & 0 & 0 & 0 & 0 & 0 & -\chi_4\bar{\alpha}_5^* \end{pmatrix}, \tag{82}$$

and

$$\boldsymbol{A}_3 = \begin{pmatrix} -\kappa & 0 & 0 & \chi_1\bar{\alpha}_1 & 0 & 0 & 0 & \chi_4\bar{\alpha}_4 \\ 0 & -\kappa & \chi_2\bar{\alpha}_1^* & 0 & 0 & 0 & \chi_4\bar{\alpha}_4^* & 0 \\ 0 & \chi_1\bar{\alpha}_1 & -\kappa & 0 & 0 & \chi_2\bar{\alpha}_2 & 0 & 0 \\ \chi_1\bar{\alpha}_1^* & 0 & 0 & -\kappa & \chi_2\bar{\alpha}_2^* & 0 & 0 & 0 \\ 0 & 0 & 0 & \chi_2\bar{\alpha}_2 & -\kappa & 0 & 0 & \chi_3\bar{\alpha}_3 \\ 0 & 0 & \chi_2\bar{\alpha}_2^* & 0 & 0 & -\kappa & \chi_3\bar{\alpha}_3^* & 0 \\ 0 & \chi_4\bar{\alpha}_4 & 0 & 0 & 0 & \chi_3\bar{\alpha}_3 & -\kappa & 0 \\ \chi_4\bar{\alpha}_4^* & 0 & 0 & 0 & \chi_3\bar{\alpha}_3^* & 0 & 0 & -\kappa \end{pmatrix}. \tag{83}$$

Provided the eigenvalues of the drift matrix $\bar{\boldsymbol{A}}$ have no negative real part, the system is stable and we can treat the fluctuation equations as describing an Ornstein-Uhlenbeck process [37]. This allows one to calculate the intracavity spectral correlation matrix,

$$\boldsymbol{S}(\omega) = (\bar{\boldsymbol{A}} + i\omega\mathbb{1})\bar{\boldsymbol{B}}\bar{\boldsymbol{B}}^T(\bar{\boldsymbol{A}}^T - i\omega\mathbb{1})^{-1}, \tag{84}$$

and this is related to the measurable output fluctuation spectra using the standard input-output relations for optical cavities [38]. Furthermore, it supplies us with all that is necessary to calculate the measurable extracavity quadripartite entanglement.

VII. OUTPUT FLUCTUATION SPECTRA

The same inequalities as given in Sec. III in terms of variances also hold when expressed in terms of the output spectra, and these are the quantities that can be measured in experiments. In the following, we use the notation $I_{ij}^{\text{out}}(\omega)$ (i.e., any of $I_{56}^{\text{out}}, I_{67}^{\text{out}}, I_{78}^{\text{out}}$) to represent the three output spectral correlations of the same form as the optimized expressions in Eqs. (6)–(8). In Fig. 4, we plot these three correlations as a function of frequency for our completely symmetric system for the below-threshold case (solid line) and the above-threshold case (dashed line). In both cases, the three correlations are equal; that is, $I_{56}^{\text{out}} = I_{67}^{\text{out}} = I_{78}^{\text{out}}$.

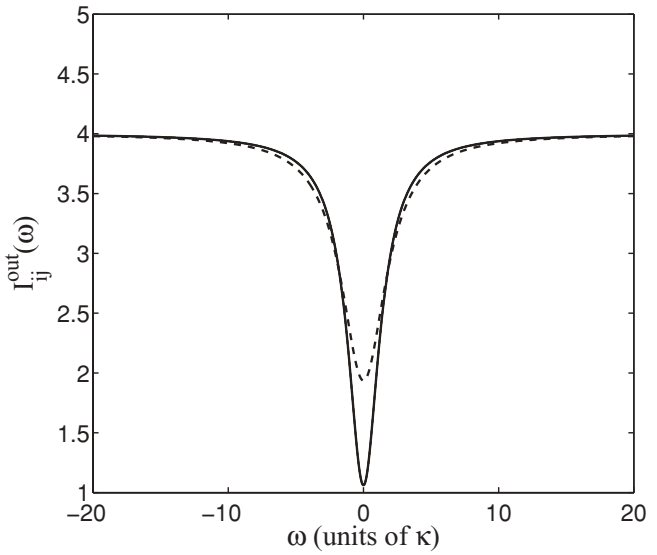

FIG. 4. The output spectral correlations, $I_{ij}^{\text{out}}(\omega)$, as a function of frequency ω (units of κ) corresponding to the quadripartite entanglement criteria given in Eqs. (21)–(23). The below-threshold (solid line) and above-threshold (dashed line) cases are shown for cavity pump amplitudes $\epsilon = 0.8\epsilon_c$ and $\epsilon = 1.2\epsilon_c$, respectively. The three correlations are equal for each case for the chosen parameters, which are symmetric with $\chi_i = \chi$, $\epsilon_i = \epsilon$, $\gamma = 10$, $\kappa = 1$, and $\chi = 10^{-2}$. All quantities plotted here and in the subsequent graph are dimensionless.

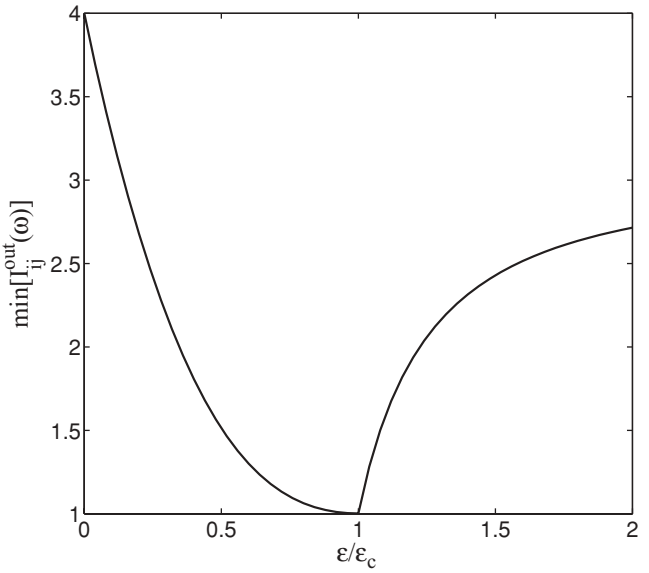

FIG. 5. Maximum quadripartite entanglement as a function of the ratio of the cavity pumping to the pumping threshold. The cavity parameters are the same as in Fig. 4, with $\gamma = 10$, $\kappa = 1$, and $\chi = 10^{-2}$. Again, all three correlations are equal for these parameters. It should be stressed that at $\epsilon/\epsilon_c = 1$ the validity of the results is limited as the linearized analysis is no longer valid.

The inequalities are violated both below and above the threshold, demonstrating quadripartite entanglement. Specifically, the results shown are for the case of the pump field amplitudes set at $\epsilon = 0.8\epsilon_c$ and $\epsilon = 1.2\epsilon_c$. For these parameter choices, the largest violation of the VLF entanglement criteria, and thus the maximum quadripartite entanglement, is for the low-frequency modes below threshold. In general, for both cases the largest degree of violation of the inequalities is observed near zero frequency. For large frequencies $I_{ij}^{\text{out}}(\omega) \to 4$, which is the uncorrelated limit for our optimized expressions.

We also determine the maximum quadripartite entanglement for the same parameters as in Fig. 4, but for a range of pump field amplitudes on both sides of the oscillation threshold. This is shown in Fig. 5, where we plot the minimum value of the output spectra at any frequency, as a function of ϵ/ϵ_c. As expected [39,40], we observe the maximum quadripartite entanglement at the critical pumping amplitude, with the caveat that the linearized fluctuation analysis is not valid in the immediate vicinity of the threshold. The fact that a gradual slope is observed below threshold in the region of maximum entanglement could prove useful for future experimental realizations of this scheme. It is also found that quadripartite entanglement persists well above threshold, with a large violation of the VLF criteria still present as the pumping is increased above the critical pumping value. In particular, well above threshold the minimum of $I_{ij}^{\text{out}}(\omega)$ approaches 3. This behavior is also seen in [39,40], where the equivalent correlations also asymptote to a finite value.

VIII. CONCLUSIONS AND OUTLOOK

We have demonstrated intracavity continous-variable quadripartite entanglement in quadruply concurrent down-conversion, both above and below the critical pumping threshold, using optimized VLF criteria. Above threshold, the proposed scheme produces a source of bright entangled output beams. The below-threshold regime provides the greatest degree of entanglement and a region where this entanglement could be measured in experiments. One of the advantages of this type of scheme lies in the number of different regimes that can be explored by tuning various parameters in experiments. For example, the pump intensities and coupling strengths can be tuned and this makes it possible to vary the degree of entanglement in the system.

Throughout this article, we have studied the properties of the interaction Hamiltonian, presented the full quantum equations of motion and performed a linearized fluctuation analysis. All results indicate that this system is a good candidate for the demonstration of quadripartite CV entanglement. In relation to experimental implementation of the scheme presented here, stabilizing a single cavity in which four entangled modes are created may prove preferable in some applications rather than alternative schemes which rely on stabilizing and synchronizing multiple OPOs.

Finally, this result could be of further significance in a similar system where one of the nonlinear couplings is absent. Such a system may be a candidate for realizing the simplest four-node cluster state [26,27].

ACKNOWLEDGMENTS

S.L.W.M. and M.K.O. are supported by the Australian Research Council Centre of Excellence for Quantum-Atom

Optics. S.L.W.M. would also like to thank the AFUW for providing financial support. A.S.B. is supported by the New Zealand Foundation for Research, Science, and Technology under Contract No. UOOX0801. O.P. is supported by U.S. National Science Foundation Grant No. PHY-0855632 and No. PHY-0555522.

[1] S. L. Braunstein and P. van Loock, Rev. Mod. Phys. **77**, 513 (2005).
[2] P. van Loock and S. L. Braunstein, Phys. Rev. Lett. **84**, 3482 (2000).
[3] P. van Loock and S. L. Braunstein, Phys. Rev. Lett. **87**, 247901 (2001).
[4] J. T. Jing, J. Zhang, Y. Yan, F. G. Zhao, C. D. Xie, and K. C. Peng, Phys. Rev. Lett. **90**, 167903 (2003).
[5] T. Aoki, N. Takei, H. Yonezawa, K. Wakui, T. Hiraoka, A. Furusawa, and P. van Loock, Phys. Rev. Lett. **91**, 080404 (2003).
[6] J. Zhang, C. D. Xie, and K. Peng, Phys. Rev. A **66**, 032318 (2002).
[7] H. Yonezawa, T. Aoki, and A. Furusawa, Nature (London) **431**, 430 (2004).
[8] L.-M. Duan, G. Giedke, J. I. Cirac, and P. Zoller, Phys. Rev. Lett. **84**, 2722 (2000).
[9] R. Simon, Phys. Rev. Lett. **84**, 2726 (2000).
[10] P. van Loock and A. Furusawa, Phys. Rev. A **67**, 052315 (2003).
[11] C. Silberhorn, P. K. Lam, O. Weiss, F. Konig, N. Korolkova, and G. Leuchs, Phys. Rev. Lett. **86**, 4267 (2001).
[12] A. Furusawa, J. L. Sørensen, S. L. Braunstein, C. A. Fuchs, H. J. Kimble, and E. S. Polzik, Science **282**, 706 (1998).
[13] A. S. Coelho, F. A. S. Barbosa, K. N. Cassemiro, A. S. Villar, M. Martinelli, and P. Nussenzveig, Science **326**, 823 (2009).
[14] O. Pfister, S. Feng, G. Jennings, R. Pooser, and D. Xie, Phys. Rev. A **70**, 020302(R) (2004).
[15] J. Guo, H. Zou, Z. Zhai, J. Zhang, and J. Gao, Phys. Rev. A **71**, 034305 (2005).
[16] A. Ferraro, M. G. A. Paris, M. Bondani, A. Allevi, E. Puddu, and A. Andreoni, J. Opt. Soc. Am. B **21**, 1241 (2004).
[17] A. S. Bradley, M. K. Olsen, O. Pfister, and R. C. Pooser, Phys. Rev. A **72**, 053805 (2005).
[18] M. K. Olsen and A. S. Bradley, J. Phys. B **39**, 127 (2006).
[19] M. K. Olsen and A. S. Bradley, Phys. Rev. A **77**, 023813 (2008).
[20] X. Su, A. Tan, X. Jia, J. Zhang, C. D. Xie, and K. C. Peng, Phys. Rev. Lett. **98**, 070502 (2007).
[21] J. F. Wang, X. Q. Yu, Y. B. Yu, P. Xu, Z. D. Xie, H. Y. Leng, and S. N. Zhu, Opt. Commun. **282**, 253 (2009).
[22] J. F. Wang, J. S. Zhao, H. Y. Leng, X. Q. Yu, Z. D. Xie, Y. L. Yin, P. Xu, and S. N. Zhu, Opt. Commun. **282**, 3729 (2009).
[23] H. Y. Leng, J. F. Wang, Y. B. Yu, X. Q. Yu, P. Xu, Z. D. Xie, J. S. Zhao, and S. N. Zhu, Phys. Rev. A **79**, 032337 (2009).
[24] N. C. Menicucci, S. T. Flammia, H. Zaidi, and O. Pfister, Phys. Rev. A **76**, 010302(R) (2007).
[25] R. C. Pooser and O. Pfister, Opt. Lett. **30**, 2635 (2005).
[26] H. Zaidi, N. C. Menicucci, S. T. Flammia, R. Bloomer, M. Pysher, and O. Pfister, Laser Phys. **18**, 659 (2008).
[27] N. C. Menicucci, S. T. Flammia, and O. Pfister, Phys. Rev. Lett. **101**, 130501 (2008).
[28] S. T. Flammia, N. C. Menicucci, and O. Pfister, J. Phys. B **42**, 114009 (2009).
[29] N. C. Menicucci, P. van Loock, M. Gu, C. Weedbrook, T. C. Ralph, and M. A. Nielsen, Phys. Rev. Lett. **97**, 110501 (2006).
[30] M. Pysher, A. Bahabad, P. Peng, A. Arie, and O. Pfister, Opt. Lett. **35**, 565 (2010).
[31] M. D. Reid, Phys. Rev. A **40**, 913 (1989).
[32] D. F. Walls and G. J. Milburn, *Quantum Optics* (Springer, Berlin, 1994).
[33] P. D. Drummond and C. W. Gardiner, J. Phys. A **13**, 2353 (1980).
[34] C. W. Gardiner, *Quantum Noise* (Springer, Berlin, 1991).
[35] R. J. Glauber, Phys. Rev. **131**, 2766 (1963).
[36] E. C. G. Sudarshan, Phys. Rev. Lett. **10**, 277 (1963).
[37] C. W. Gardiner, *Handbook of Stochastic Methods* (Springer, Berlin, 2002).
[38] C. W. Gardiner and M. J. Collett, Phys. Rev. A **31**, 3761 (1985).
[39] M. K. Olsen, A. S. Bradley, and M. D. Reid, J. Phys. B **39**, 2515 (2006).
[40] N. Olivier and M. K. Olsen, Opt. Commun. **259**, 781 (2006).